**Supplemental Table 1. List of antibodies used.**

| Antibody name | Catalog number | Manufacturer |
|---|---|---|
| **Anti-α-SMA antibody** | ab7817 | Abcam |
| **Anti-Collagen I antibody** | ab270994 | Abcam |
| **Anti-ZO1 tight junction protein antibody** | ab221547 | Abcam |
| **Anti-MUC2 antibody** | ab272692 | Abcam |

**Supplemental Table 2. Primer sequences used for Real-time PCR analysis.**

| Gene name | Forward Sequence (5'-3') | Reverse Sequence (5'-3') |
|---|---|---|
| **Gapdh** | TGGTGAAGCAGGCATCTGAG | TGCTGTTGAAGTCGCAGGAG |
| **α-SMA** | TTCCTTCGTGACTACTGCCG | TATAGGTGGTTTCGTGGATGCC |
| **Collagen I** | CTGGCGGTTCAGGTCCAAT | TTCCAGGCAATCCACGAGC |
| **Collagen III** | CTGGTCAGCCTGGAGATAAG | ACCAGGACTACCACGTTCAC |
| **TGF-β** | CCACCTGCAAGACCATCGAC | CTGGCGAGCCTTAGTTTGGAC |
| **IL-17** | TCAGCGTGTCCAAACACTGAG | CGCCAAGGGAGTTAAAGACTT |
| **Fibronectin** | ATGTGGACCCCTCCTGATAGT | GCCCAGTGATTTCAGCAAAGG |
| **IL-6** | TCTATACCACTTCACAAGTCGGA | GAATTGCCATTGCACAACTCTTT |
| **TNF-α** | CAGGCGGTGCCTATGTCTC | CGATCACCCCGAAGTTCAGTAG |
| **PPARγ** | TCGCTGATGCACTGCCTATG | GAGAGGTCCACAGAGCTGATT |
| **ZO-1** | GCCGCTAAGAGCACAGCAA | GCCCTCCTTTTAACACATCAGA |
| **MUC-2** | AGGGCTCGGAACTCCAGAAA | CCAGGGAATCGGTAGACATCG |

**Supplemental Figure 1. Correlation analysis of *Bifidobacterium*, *Blautia* and *Streptococcus* with clinical symptoms.**

The patients were divided into the elderly group and the young group according to the age of 60. In the young group, *Bifidobacterium* and *Blautia* were positively correlated with FVC, and *Bifidobacterium* was positively correlated with FEV. However, there was no statistically significant difference in the correlation between *Bifidobacterium* or *Blautia* and symptoms in the elderly group.

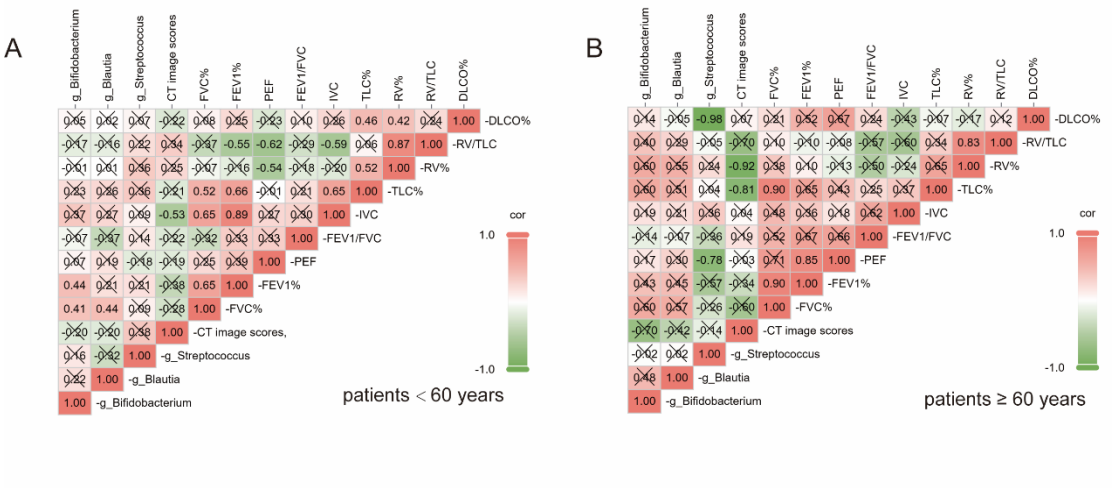


Supplemental Figure 1. A: Correlation among abundance of *g_Bifidobacterium*, *g_Blautia* and *g_Streptococcus* in the gut and clinical symptoms in the younger. B. Correlation among abundance of *g_Bifidobacterium*, *g_Blautia* and *g_Streptococcus* in the gut and clinical symptoms in the elderly. The unlabeled ones are $P < 0.05$.

**Supplemental Figure 2. *B. adolescentis* reduced mortality and improved inflammation in pulmonary fibrosis.**

Body weight measurements revealed no significant differences among the three experimental groups following 14 days of *B. adolescentis* administration in aging mice (Supplemental Figure 2A), indicating no adverse effects of the probiotic treatment. The mice in NC group survived the 14-day observation period, while mortality commenced at day 6 in PF group and day 7 in BA group (Supplemental Figure 2B). As shown in Supplemental Figure 2, C and D, BLM-induction markedly elevated pro-inflammatory cytokines (IL-6, TNF-α) in BALF (Supplemental Figure 2, C-D), with *B. adolescentis* significantly attenuating these responses. Similar patterns were observed in young mice (Supplemental Figure 2, E-G), where BLM-induced inflammation was progressively exacerbated by day 14 but effectively ameliorated after *B. adolescentis* intervention.

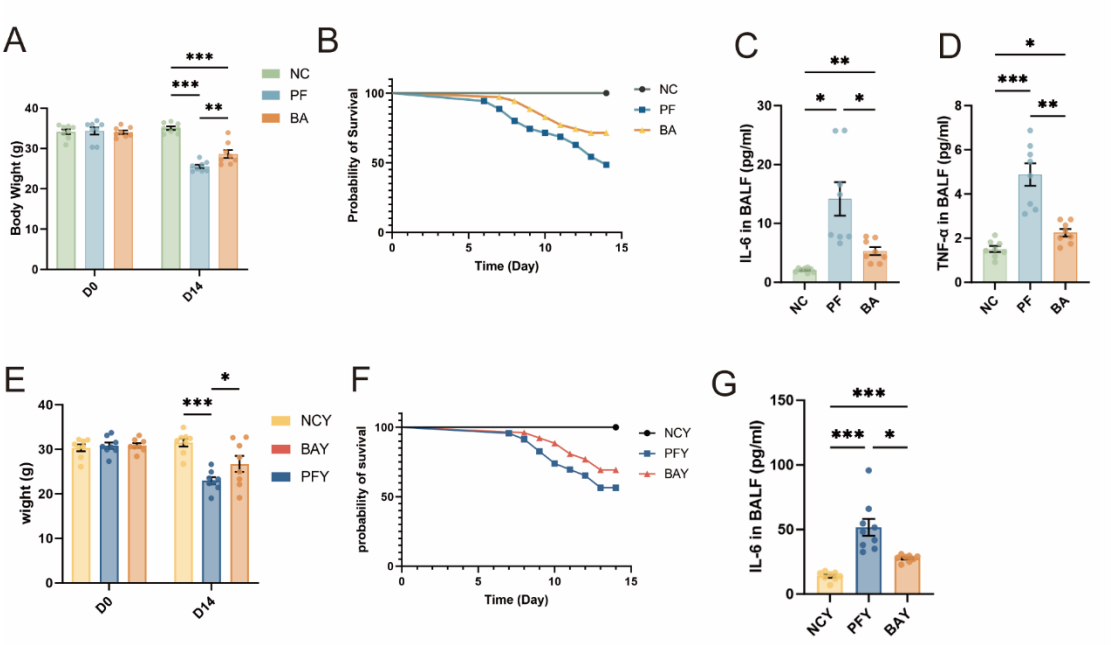


Supplemental Figure 2. A: Bar charts of body weight of aging mice before modeling and 14 days after modeling. B: Line graph of the body weight of aging mice. C-D: IL-6 and TNF-α in BALF of aging mice. E: Bar charts of body weight of young mice before modeling and 14 days after modeling. F: Line graph of the body weight of young mice. G: IL-6 in BALF of young mice. * *P* <*0.05*, ** *P* <*0.01*, *** *P* <*0.001*.

**Supplemental Table 3. Daily mortality rate statistics using chi-square test for proportions.**

| | PF group | PFY group | BA group | BAY group | *P* value |
|---|---|---|---|---|---|
| Day6 | 5.70% | 0.00% | 0.00% | 0.00% | 0.252 |
| Day7 | 11.40% | 4.30% | 2.90% | 0.00% | 0.227 |
| Day8 | 20.00% | 8.70% | 5.70% | 3.80% | 0.128 |
| Day9 | 25.70% | 17.40% | 11.40% | 7.70% | 0.223 |
| Day10 | 28.60% | 26.10% | 17.10% | 11.50% | 0.369 |
| Day11 | 31.40% | 30.40% | 22.90% | 19.20% | 0.677 |
| Day12 | 37.10% | 34.80% | 25.70% | 23.10% | 0.604 |
| Day13 | 45.70% | 43.50% | 28.60% | 30.80% | 0.398 |
| Day14 | 51.40% | 43.50% | 28.60% | 30.80% | 0.187 |

**Supplemental Figure 3. *B. adolescentis* improves the down-regulation of fibrosis-related gene expression.**

We examined the relative expression levels of Collagen III, and Fibronectin of pulmonary. As shown in Supplemental Figure 3, A-D, that their levels were significantly increased in the PF and PFY group and downregulated after *B. adolescentis* intervention (all $P < 0.05$).

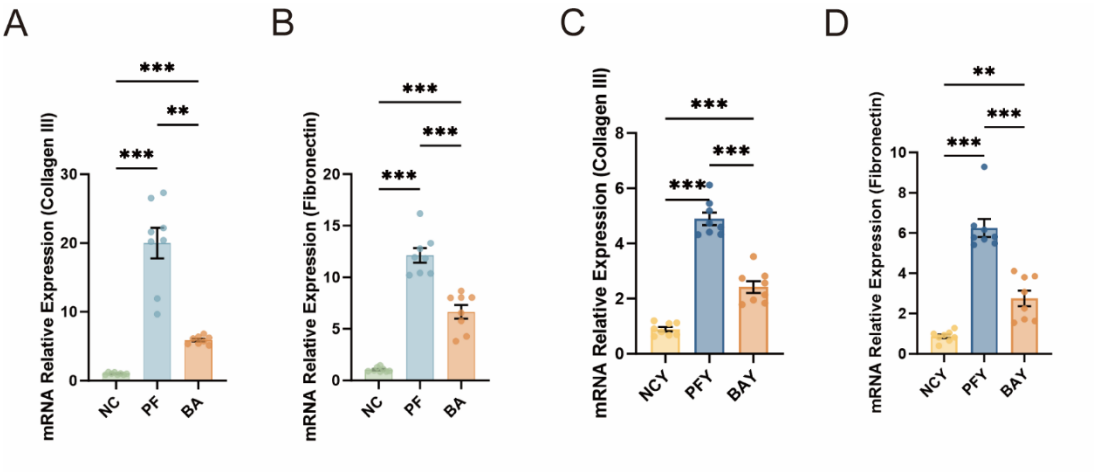


Supplemental Figure 3. A-B: mRNA relative expression of Collagen III, and Fibronectin in aging mice. C-D: mRNA relative expression ofCollagen III, and Fibronectin in young mice. * *P <0.05*, ** *P <0.01*, *** *P <0.001*.

**Supplemental Figure 4. The differentially expressed genes in the three groups**

In the Venn diagram we can see the number of differentially expressed genes in each group.

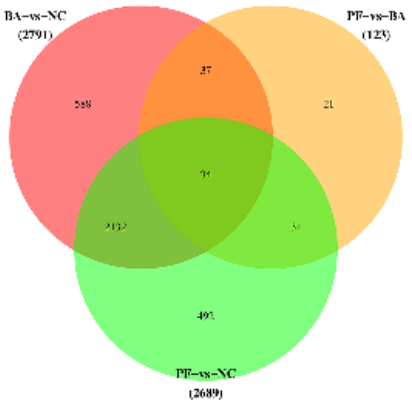


Supplemental Figure 4: A: Venn diagrams of transcriptional genes in each group.

**Supplemental Figure 5. *B. adolescentis* reshaped the gut microbiota structure**

In Supplemental Figure 4, A-D, the 16s results of the colons of aging mice and young mice indicated that the intervention with *B. adolescentis* improved the structure and abundance of the intestinal microbiota in mice with pulmonary fibrosis. LEfSe analysis was performed to search for meaningful biomarkers between groups. Using Linear Discriminant Analysis (LDA), feature taxa with significant differences in abundance were identified, and with LDA score > 2 were shown (Supplemental Figure 4, E and F). From genus level, the abundance of *Ligilactobacillus*, *Prevotella*, *Bacteroides*, *Parabacteroides*, *Clostridium*, *Oscillospira*, *Paludicola*, and *Barnesiella* were significantly increased in PF group (PF vs. NC). From family level, the abundance of *Prevotellaceae*,

*Bacteroidaceae*, *Rikenellaceae*, *Eubacteriaceae*, *Rhodospirillaceae*, *Enterococcaceae*, *Mycoplasmataceae*, *Flavobacteriaceae* were significantly increased in PF group (PF vs. NC). And after *B. adolescentis* intervention, compared with PF group, the abundance of *Desulfovibrio*, *Turicibacte* and *Bifidobacterium* increased significantly at the genus level, and the abundance of *Desulfovibrionaceae*, *Peptostreptococcaceae* and *Bifidobacteriaceae* were significantly increased at the famliy level. As shown in Supplemental Figure 4, G and H, the BAY group significantly increased *Helicobacter*, *Firmicutes*, *Campylobacter*, *Deferribacter*, and *Enterobacteriaceae.* PFY group significantly increased *Lachnospiraceae*, *Proteobacteria*, *Prevotella*, *Burkholderiaceae*, etc. In Supplemental Figure 4I, compareing with the BAY group and BA group, the abundances of *Lachnospira*, *Prevotella*, *Bacteroides*, *Parabacteroides*, and *Ligilactobacillus* decreased, and the abundances of *Helicobacter*, *Dubosiella*, *Allobaculum*, *Rikenella*, *Roseburia*, *Mucispirillum*, *Desulfovibrio*, and *Actinobacteria* have increased. In Supplemental Figure 4J, the comparison between the BA group and the BAY group revealed that *Bifidobacterium*, *Turicibacter*, and *norank_f_Desulfovibrionaceae* were more abundant in the BA group. And comparing with PF group and PFY group, we found that *Ligilactobacillus* was not only a microbiote that increased in both groups after BLM induction, but also the abundance of *Ligilactobacillus* in the PF group of aging mice was significantly higher than that in the PFY group.

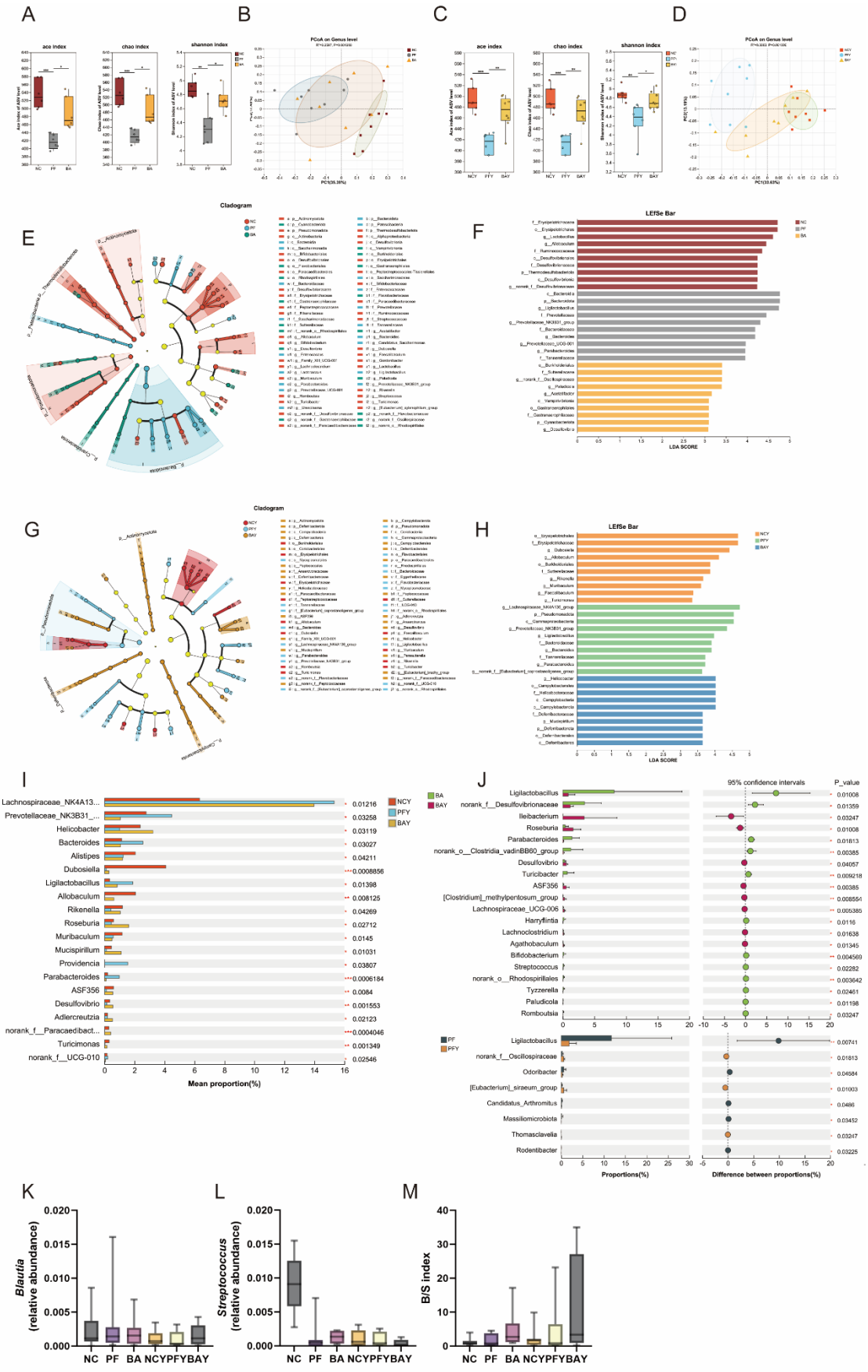


Supplemental Figure 5. A: α-diversity index analysis of aging mice, the left is the ace index, the middle is the

chao index, and the right is the shannon index. B: β-diversity, principal co-ordinates analysis (PCoA) of aging mice. C: α-diversity index analysis of young mice, the left is the ace index, the middle is the chao index, and the right is the shannon index. D: β-diversity, PCoA of young mice. E-F: LEfSe analyzes multi-level species hierarchy tree diagrams of aging mice and Linear Discriminant Analysis (LDA), with the LDA score > 2. G-H: LEfSe analyzes multi-level species hierarchy tree diagrams of young mice and LDA, with the LDA score > 2. I: Bar charts of differential bacteria in the genus level among the three groups of young mice. J: Comparative analysis between BA group and BAY group in genus level (upper part), and comparative analysis between PF group and PFY group in genus level (lower part). K-L: Relative abundance of *Blautia* and *Streptococcus*. M. B/S index in aging mice and young mice. * $P < 0.05$, ** $P < 0.01$, *** $P < 0.001$.

**Supplemental Figure 6. Correlation analysis of gut microbiota and metabolites**

PCA analysis indicated that the metabolomic results of the tissues induced by BLM were completely different from those of healthy mice, and the metabolic results changed after *B. adolescentis* intervention (Supplemental Figure 5A). Partial Least Squares Discriminant Analysis (PLS-DA) further proved that there was significant variability between the other two groups in the PF group, and BLM disrupted the metabolic profile of lung tissue after induction (Supplemental Figure 5B). We conducted a correlation analysis between the important metabolites and the top 20 differential microbiota of aging mice (Supplemental Figure 5C). We found that the metabolic substances with a greater correlation to the microbiota were Pe(P-18:0/0:0), Linoleoyl Carnitine, Suberic Acid, Azelaic Acid, 13,14-Dihydro-15-Keto Prostaglandin E2, 15-Deoxy-Delta 12,14 -Prostaglandin J2, 16-Phenyl Tetranor Prostaglandin E1, Prostaglandin E2.

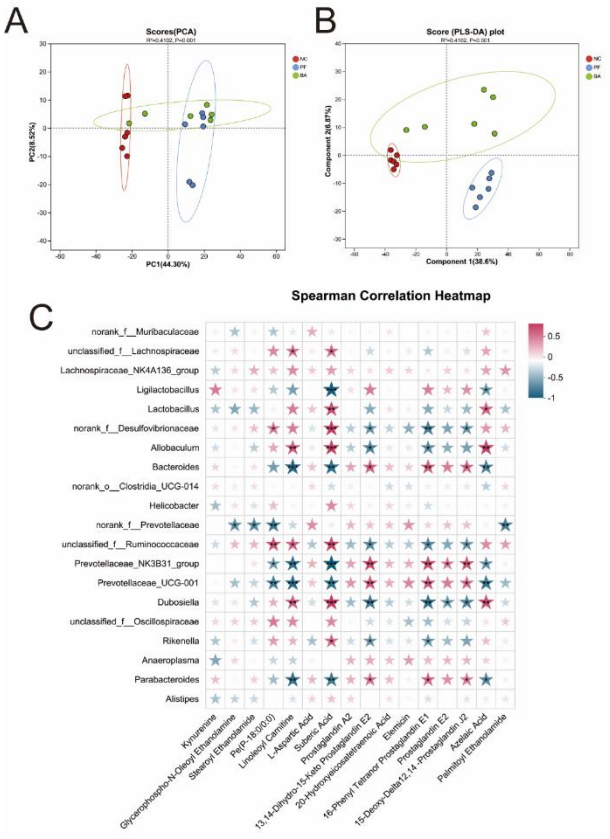


Supplemental Figure 6. A: PCA analysis results. B: Partial Least Squares Discriminant Analysis (PLS-DA). C: Correlation analysis of intestinal microbiota and metabolites. Heat map of correlation analysis between top 20 intestinal microbiota and key metabolites* $P < 0.05$, ** $P < 0.01$, *** $P < 0.001$.